



HAL
open science

An insight into grain interaction in bentonite/claystone mixtures

Zhixiong Zeng, Yu-Jun Cui, Jean Talandier

► **To cite this version:**

Zhixiong Zeng, Yu-Jun Cui, Jean Talandier. An insight into grain interaction in bentonite/claystone mixtures. *Acta Geotechnica*, 2022, 18, pp.573-579. 10.1007/s11440-022-01553-1 . hal-04181894

HAL Id: hal-04181894

<https://enpc.hal.science/hal-04181894v1>

Submitted on 16 Aug 2023

HAL is a multi-disciplinary open access archive for the deposit and dissemination of scientific research documents, whether they are published or not. The documents may come from teaching and research institutions in France or abroad, or from public or private research centers.

L'archive ouverte pluridisciplinaire **HAL**, est destinée au dépôt et à la diffusion de documents scientifiques de niveau recherche, publiés ou non, émanant des établissements d'enseignement et de recherche français ou étrangers, des laboratoires publics ou privés.

1 **An insight into grain interaction in bentonite/claystone mixtures**

2
3 Zhixiong Zeng^{1*}, Yu-Jun Cui¹, Jean Talandier²

4
5 1: Laboratoire Navier/CERMES, Ecole des Ponts ParisTech, 6 et 8 avenue Blaise Pascal, 77455
6 Marne La Vallée cedex 2, France

7 2: Andra, 1/7, rue Jean Monnet, 92298 Châtenay-Malabry cedex, France

8
9
10
11
12
13 ***Corresponding author**

14 Zhixiong Zeng

15 Ecole des Ponts ParisTech

16 6–8 av. Blaise Pascal, Cité Descartes, Champs-sur-Marne

17 77455 Marne-la-Vallée cedex 2

18 France

19 Tel.: +33 781926608

20 Fax: +33 164153562

21 E-mail address: zhixiong.zeng@enpc.fr

22 **Abstract:** This paper investigates the swelling mechanism of Callovo-Oxfordian (COx) claystone
23 grain in its mixtures with bentonite which are potential candidate for engineered barriers in the
24 French high-level radioactive waste disposal. The swelling pressures of MX80 bentonite/COx
25 claystone mixtures with various bentonite fractions and dry densities were first experimentally
26 determined by carrying out infiltration tests under constant-volume conditions. According to the
27 experimental results, the claystone void ratio after hydration in the mixtures was estimated by
28 taking into account the bentonite–claystone grain interaction. Then, the volume change of
29 claystone grain under different pressures applied by swollen bentonite was determined. The
30 volumetric strain of claystone grain was found to decrease linearly with the increase of pressure.
31 This allowed the indirect determination of the swelling pressure of claystone grain. The
32 determined value was found to be comparable to that estimated from the relationship between the
33 void ratio and the swelling pressure in the direction perpendicular to the stratification of intact
34 COx claystone, confirming the identified swelling mechanism of bentonite/claystone mixtures.

35

36 **Keywords:** bentonite/claystone mixture; claystone void ratio; volumetric strain; swelling pressure
37 of claystone grain

38 **List of symbols**

39 B bentonite fraction

40 e void ratio

41 e_c claystone void ratio

42 e_c^0 initial void ratio of claystone grain

43 G_{sc} specific gravity of claystone

44 K_0 earth pressure coefficient at rest

45 OCR over-consolidation ratio

46 P_s measured global swelling pressure of mixture

47 $P_{s\text{-mean}}$ mean swelling pressure of claystone

48 $P_{s\text{-per}}$ swelling pressure in the direction perpendicular to the stratification of intact claystone

49 ρ_w water unit mass

50 ρ_{db} bentonite dry density

51 ρ_{dc} claystone dry density

52 ρ_{dc}^0 initial claystone dry density

53 ρ_{dm} mixture dry density

54 ε_v claystone volumetric strain of claystone

55 φ_c effective internal friction angle

56 **1 Introduction**

57 The French Radioactive Waste Management Agency (Andra) is currently envisaging to construct a
58 geological repository for high-level radioactive waste in the Callovo-Oxfordian (COx) claystone
59 formation [1]. The disposal galleries are planned to be excavated at a depth of 490 m in the 150-m-
60 thick layer of COx claystone. To seal or backfill these galleries after the emplacement of waste
61 canisters, pure bentonite or bentonite/sand mixture may be employed. To reduce the excavation
62 wastes and to have lower costs, excavated COx claystone has been proposed to partially or completely
63 replace the commercial bentonite as sealing/backfilling material. Once the galleries are closed, the
64 crushed claystone or its mixture with bentonite is expected to exhibit a swelling pressure high enough
65 to stabilize the surrounding rock mass [7, 13, 18].

66 Over the last few decades, the swelling pressure of pure bentonite and bentonite/sand mixtures
67 were widely studied [3-5, 9]. It was found that the swelling pressure increased linearly with the
68 increase of dry density in a semi-logarithmic plane. Additionally, for each specific bentonite, the
69 relationship between the swelling pressure and the final bentonite dry density could be described by
70 a unique relationship, regardless of sand fraction [2, 11]. The swelling pressure of bentonite/sand
71 mixtures was principally dominated by the matrix of bentonite, while the sand grains remained inert
72 without any contribution to the global swelling pressure. Unlike the inert sand, the COx claystone
73 contains a significant amount of clay minerals. Upon contact with water, both the bentonite and
74 claystone grains adsorbed water and the interaction between them could occur. Zeng et al. [13] argued
75 that the swelling of claystone was conditioned by the swollen bentonite due to the much higher
76 swelling capacity of bentonite. However, this swelling mechanism of claystone grain in its mixtures

77 with bentonite has not been analysed in-depth.

78 In this paper, a series of constant-volume swelling pressure tests were performed on the MX80
79 bentonite/COx claystone mixtures with various bentonite fractions and dry densities. By considering
80 the interaction between bentonite and claystone in the development of global swelling pressure, the
81 claystone void ratio in the mixture after hydration was calculated and the relationship between the
82 claystone grain volume change and the pressure applied by swollen bentonite was determined.
83 Subsequently, the swelling pressure of crushed claystone grains was indirectly determined and then
84 compared with that estimated from the measured swelling pressure in the direction perpendicular to
85 the stratification of intact COx claystone.

86 **2 Materials and methods**

87 The mixtures of MX80 bentonite and COx claystone powders were used in this study. The MX80
88 bentonite was taken from Wyoming, USA. Prior to the experiment, the bentonite was crushed to
89 powders with a maximum grain size of 2.0 mm. The COx claystone was extracted from the Bure
90 Underground Research Laboratory. The subsequent processing of excavated COx claystone
91 comprised the crushing and sieving passing through 2.0 mm sieve. The grain size of processed COx
92 claystone powders used in this work is in the range of 0.08-2.0 mm. The grain size distributions of
93 the bentonite and claystone determined by dry-sieving method are shown in Fig. 1. The mean particle
94 sizes D_{50} of the bentonite and claystone powders are 0.55 and 0.58 mm, respectively. The physico-
95 chemical properties of the tested materials are listed in Table 1. The initial suctions of the bentonite
96 and claystone powders were also measured by hygrometer WP4, equal to 101 and 27 MPa,
97 respectively. Using a pycnometer with a non-aromatic hydrocarbon fluid (Kerdane), the apparent

98 volume of soil grains at a given dry mass was measured and the respective average dry densities of
 99 bentonite and claystone grains were thus determined, equal to 2.00 and 2.31 Mg/m³.

100 **Table 1** Physico-chemical properties of MX80 bentonite and COx claystone

Soil property	MX80 bentonite	COx claystone
Water content (%)	11.4	6.1
Specific gravity	2.76	2.70
Liquid limit (%)	494	41
Plastic limit (%)	46	24
Clay-size fraction (%)	86	26
Main clay minerals	Smectite	Interstratified illite-smectite

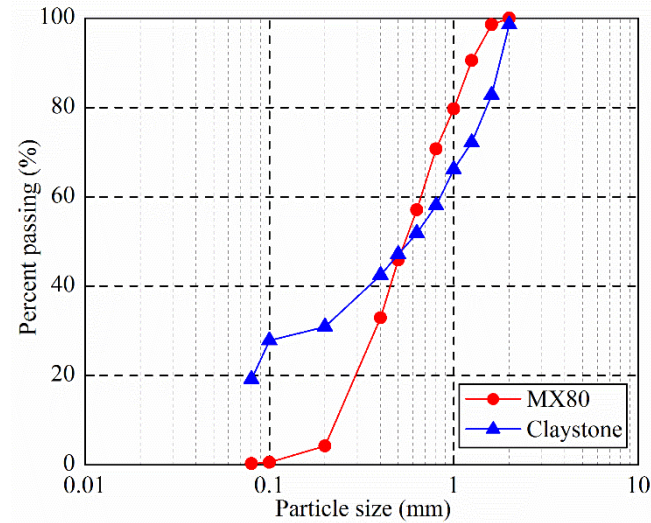
101 The bentonite and claystone powders at various proportions of 70/30, 50/50, 30/70, 20/80, 10/90
 102 in dry mass were first mixed thoroughly. As shown in Table 2, the corresponding bentonite fractions
 103 (*B*) of the mixtures were 70, 50, 30, 20 and 10%. Subsequently, the mixtures and pure claystone were
 104 statically compacted at a control rate of 0.05 mm/min to reach various target dry densities. The
 105 diameter and height of the compacted samples were 50 and 10 mm, respectively. After compaction,
 106 the samples were transferred to the stainless steel cell (50 mm in diameter) and the two sides of
 107 samples were covered by two filter papers and two porous discs (Fig. 2). At the top, the samples were
 108 restrained by a piston blocked using screws. Synthetic site water was injected from the bottom of the
 109 cell at constant water head of about 1 m (the corresponding water pressure was about 10 kPa). The
 110 synthetic site water has the same chemical composition as the site water in Bure and it was prepared
 111 by mixing the relevant chemical components (Table 3) with de-ionized water until full dissolution.
 112 The samples were hydrated under constant-volume conditions and the expelled air/water flowed
 113 through the air/water outlets at the top. During the hydration, the vertical force was monitored using
 114 a force transducer (accuracy ± 0.01 kN) installed under the cell. Note that the maximum vertical

115 displacement of the apparatus was quite small, estimated at 0.0049 mm. Thus, the volume change of
 116 samples due to the deformation of apparatus was ignored.

117 **Table 2** Test program and main results

Test No.	Bentonite fraction B (%)	Dry density of sample ρ_{dm} (Mg/m ³)	Initial water content w_m (%)	Claystone void ratio e_c	Volumetric strain of claystone grain ε_v (%)	Final swelling pressure P_s (MPa)
S01	70	1.38	9.8	0.08	-7.8	0.43
S02	70	1.50	9.8	0.13	-2.9	1.11
S03	70	1.63	9.8	0.07	-8.1	2.53
S04	70	1.71	9.8	0.02	-12.4	3.94
S05	50	1.27	8.8	0.49	27.4	0.13
S06	50	1.56	8.8	0.30	11.5	0.85
S07	50	1.73	8.8	0.18	1.1	2.10
S08	50	1.76	8.8	0.19	2.2	2.91
S09	30	1.50	7.7	0.18	26.2	0.22
S10	30	1.60	7.7	0.47	20.6	0.46
S11	30	1.68	7.7	0.41	16.4	0.78
S12	30	1.79	7.7	0.36	10.8	1.59
S13	30	1.89	7.7	0.30	5.0	2.72
S14	30	1.99	7.7	0.23	0.9	5.23
S15	20	1.60	7.2	0.18	27.3	0.26
S16	20	1.69	7.2	0.49	20.5	0.44
S17	20	1.77	7.2	0.41	15.8	0.70
S18	20	1.88	7.2	0.35	11.8	1.93
S19	10	1.61	6.6	0.31	33.7	0.14
S20	10	1.68	6.6	0.56	28.7	0.23
S21	10	1.78	6.6	0.50	21.5	0.39
S22	10	1.90	6.6	0.42	15.5	1.07
S23	0	1.80	6.1	0.35	28.3	0.15
S24	0	1.90	6.1	0.50	21.8	0.47
S25	0	1.99	6.1	0.42	16.3	0.79

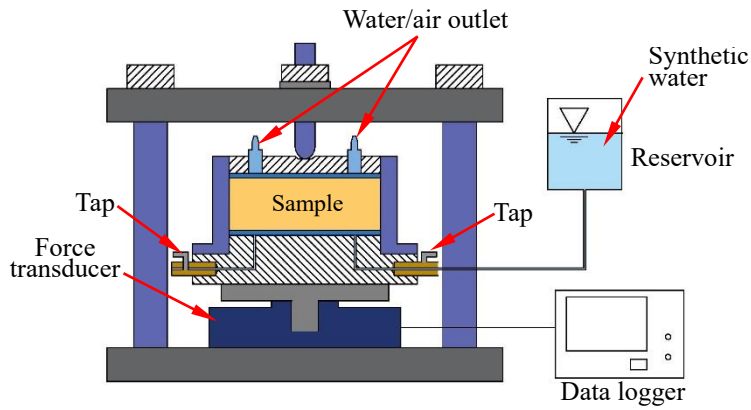
118



119

120

Fig. 1 Grain size distributions of MX80 bentonite and COx claystone



121

122

Fig. 2 Layout of the experimental setup for swelling pressure tests

123

Table 3 Chemical composition of the synthetic site water

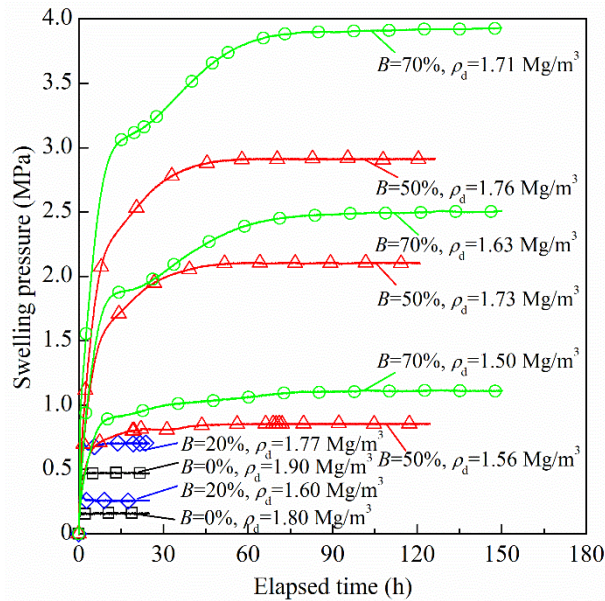
Component	NaCl	NaHCO ₃	KCl	CaSO ₄ •2H ₂ O	MgSO ₄ •7H ₂ O	CaCl ₂ •2H ₂ O	Na ₂ SO ₄
Content (g/L)	1.950	0.130	0.035	0.630	1.020	0.080	0.700

124 3 Experimental results and discussion

125 3.1 Global swelling pressure

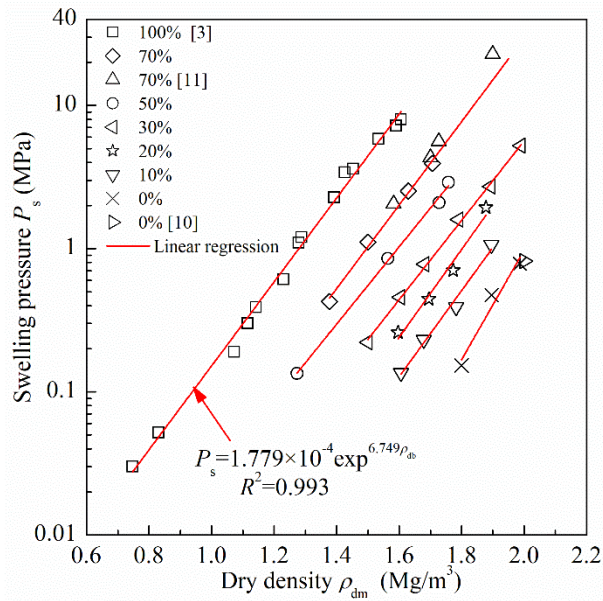
126 Fig. 3 depicts the typical evolution of the global swelling pressure of samples with various bentonite
 127 fractions and dry densities. On the whole, the global swelling pressure of the samples with high
 128 bentonite fractions (larger than 50%) and high dry densities (larger than 1.50 Mg/m³) increased with
 129 elapsed time and then tended to stabilise. By contrast, the swelling pressure of the samples with low
 130 bentonite fractions (smaller than 20%) and low dry densities (smaller than 1.77 Mg/m³) increased

131 quickly at the beginning and reached a peak. Then, it decreased and tended to stabilise.



132
133 **Fig. 3** Typical evolutions of the global swelling pressure of samples with various bentonite fractions
134 and dry densities

135 The swelling pressure tests ended after 25-150 h and the samples became saturated according
136 the results of Zeng et al. [14]. The variation of final swelling pressure with respect to the dry density
137 of samples is presented in Fig. 4 and compared with the results from other researchers [3, 10, 11]. It
138 is observed that the final swelling pressure of samples increased linearly with the increase of dry
139 density in a semi-logarithmic plane. At the same dry density, the swelling pressure of pure bentonite
140 was 100 times larger than that of pure claystone. For the bentonite/claystone mixtures, the higher the
141 bentonite fraction, the larger the final swelling pressure.



142

143

Fig. 4 Variation of the final swelling pressure with sample dry density

144

3.2 Volume change behaviour of claystone grains

145

When the bentonite/claystone mixtures were hydrated, the bentonite grains are expected to rapidly

146

swell and fill up the voids in the mixtures, thanks to their extremely high swelling capacity, while the

147

claystone grains are expected to adsorb water under the pressure applied by the swollen bentonite [13,

148

15]. This implies that the pressure at the interface of bentonite and claystone was governed by the

149

bentonite property. Note that the water pressure was quite low and the pressure at the interface of

150

bentonite and claystone could be considered as an effective stress. To clarify the role of the claystone

151

in the mixture, an additional assumption was made: the pressure at the interface of bentonite and

152

claystone was equal to the global swelling pressure (Fig. 5a and b), as suggested by Yang et al. [12]

153

when dealing with the consolidation behaviour of a lumpy granular soil under one-dimensional

154

condition. Thereby, given the measured global swelling pressure of mixture (P_s in MPa), the final

155

bentonite dry density in the mixture (ρ_{db} in Mg/m^3) can be estimated according to the relationship

156

between the swelling pressure and the final dry density of pure bentonite (Fig. 4):

157
$$P_s = 1.779 \times 10^{-4} \exp^{6.749\rho_{db}} \quad (1)$$

158 Based on the binary composition of the mixture, the final claystone dry density (ρ_{dc} in Mg/m^3) in the
 159 mixture can be deduced using Eq. (2):

160
$$\rho_{dc} = \frac{\rho_{db}\rho_{dm}(1-B/100)}{\rho_{db}-\rho_{dm}(B/100)} \quad (2)$$

161 where ρ_{dm} is the final mixture dry density (expressed in Mg/m^3) and ρ_{db} is the final bentonite dry
 162 density (expressed in Mg/m^3).

163 For pure claystone ($B=0$), the COx claystone swelled and filled up the voids between grains,
 164 becoming continuous (Fig. 5c). Thus, the final COx claystone dry density after saturation is equal to
 165 the global dry density.

166 Correspondingly, the final claystone void ratio e_c in the mixture and pure claystone can be
 167 determined:

168
$$e_c = \frac{G_{sc}\rho_w}{\rho_{dc}} - 1 \quad (3)$$

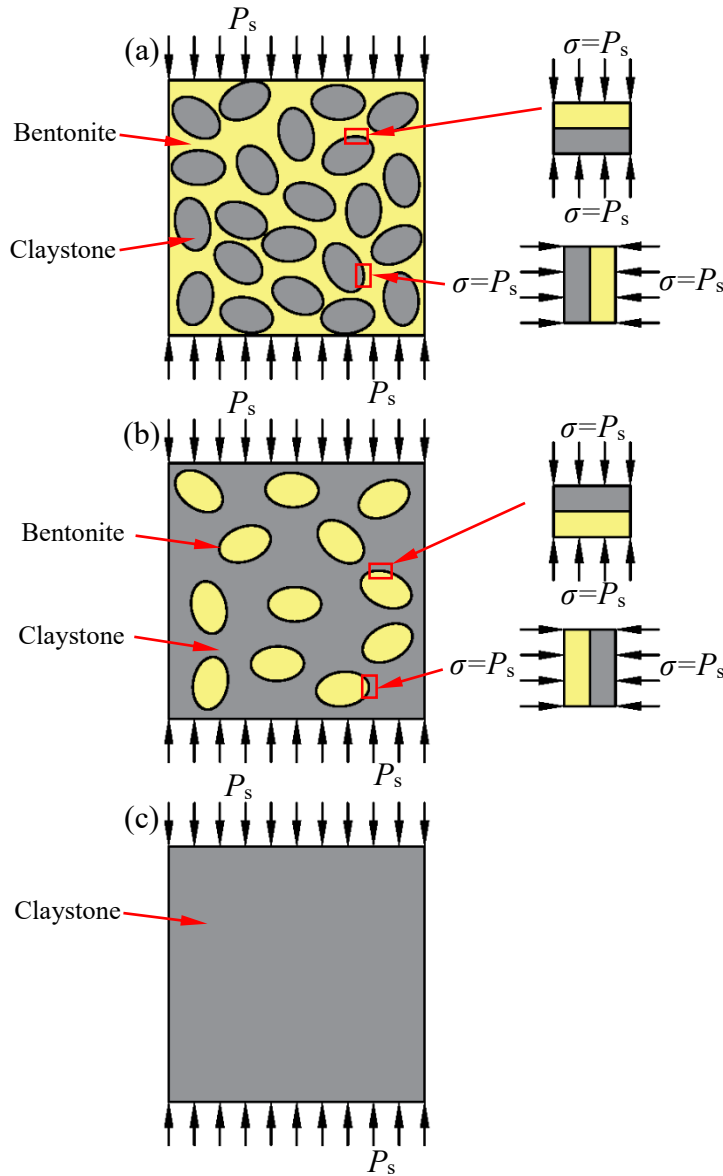
169 where G_{sc} is the specific gravity of claystone and ρ_w is the water unit mass.

170 In order to describe the volume change behaviour of claystone grain after hydration, the claystone
 171 volumetric strain (ε_v) was determined using Eq. (4):

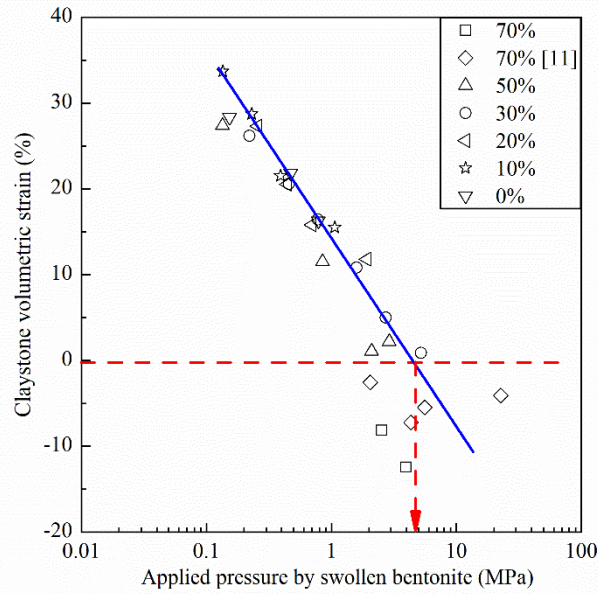
172
$$\varepsilon_v = \frac{e_c - e_c^0}{(1 + e_c^0)} = \frac{\rho_{dc}^0}{\rho_{dc}} - 1 \quad (4)$$

173 where e_c^0 is the initial void ratio of claystone grain and ρ_{dc}^0 is the initial dry density (equal to 2.31
 174 Mg/m^3). According to Eqs. (1), (2), (3) and (4), the claystone void ratios and the volumetric strains
 175 of claystone for all the samples with various bentonite fractions and dry densities were calculated and
 176 the calculated results are summarized in Table 2. For further analysis, the results of Wang et al. [11]
 177 were collected and analysed in the same fashion. Fig. 6 depicts the variation of volumetric strain with

178 the pressure applied by the swollen bentonite. It appears that the volumetric strain of claystone
 179 decreased with the increase of pressure, regardless of the bentonite fraction. Moreover, the claystone
 180 grains swelled under low pressures and collapsed under high pressures.



181
 182 **Fig. 5** Structure sketch of the samples after saturation: (a) mixtures with a large bentonite fraction,
 183 (b) mixtures with a small bentonite fraction, and (c) pure claystone. Note: the zones for bentonite
 184 and claystone after full saturation include voids in them



185
 186 **Fig. 6** Relationship between the claystone volumetric strain and the applied pressure by swollen
 187 bentonite

188 *3.3 Swelling pressure of claystone grains*

189 To further verify the swelling mechanism of claystone in its mixtures with bentonite, the swelling
 190 pressure of claystone grain was indirectly determined and then compared with that measured on intact
 191 COx claystone. According to the load-swell method, the volume changes of claystone grains
 192 subjected to various stresses were measured. This allowed the indirect determination of the swelling
 193 pressure of claystone grains. The swelling pressure corresponds to the stress at the intersection of the
 194 volumetric strain curve (represented by the blue solid line in Fig. 6) with the no volume change line
 195 (represented by the dash line in Fig. 6). A swelling pressure of about 4.9 MPa was thus determined
 196 for the claystone grain. Note that this swelling pressure referred to a mean value of those in all
 197 directions.

198 Using constant-volume, load-swell and Cui' methods, Zhang et al. [19] performed a series of
 199 swelling pressure tests on intact COx claystone, which had a similar water content to the crushed
 200 claystone powders used in this study (6.1%). They found that there was a good relationship between

201 the swelling pressure ($P_{s\text{-per}}$ in MPa) and void ratio (e) (Fig. 7):

$$202 \quad P_{s\text{-per}} = 1.365 \times 10^6 \exp^{-71.562e} \quad (5)$$

203 According to Eq. (5), the intact COx claystone with a void ratio of 0.17 corresponded to a swelling
204 pressure of 7.11 MPa. It is worth noting that this swelling pressure was measured in the direction
205 perpendicular to the stratification of claystone and did not represent the mean value. The measured
206 swelling pressure corresponded to an effective stress because the pore water pressure could be ignored
207 during the testing [17]. Moreover, in the swelling pressure test, the intact claystone was placed in
208 oedometer cell and it swelled under zero lateral deformation condition or K_0 condition. According to
209 the empirical relationship proposed by Mayne & Kulhawy [6], the earth pressure coefficient at rest
210 K_0 (ratio of horizontal and vertical effective stresses) for over-consolidated soil can be estimated using
211 Eq. (6):

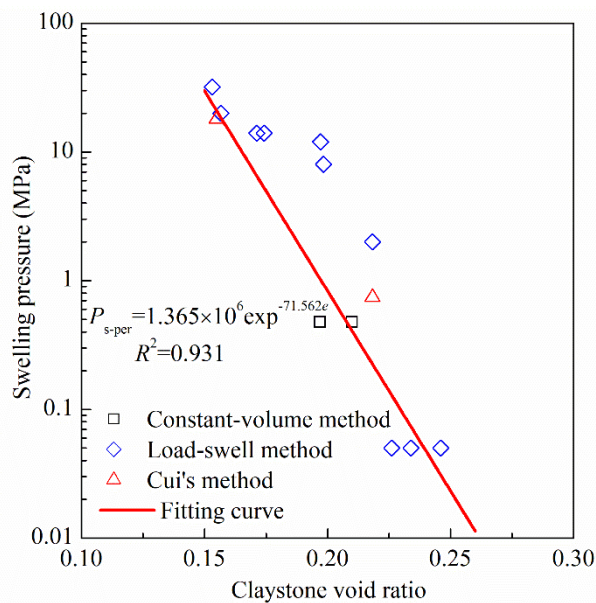
$$212 \quad K_0 = (1 - \sin \varphi_c) \text{OCR}^{\sin \varphi_c} \quad (6)$$

213 where OCR and φ_c are the over-consolidation ratio and the effective internal friction angle,
214 respectively. The over-consolidation ratio is defined as the ratio of pre-consolidation stress to the
215 current vertical stress. Based on the results from oedometer compression test on intact COx claystone,
216 in which the loading direction was perpendicular to the stratification of claystone [8], the pre-
217 consolidation stress was estimated at 8.5 MPa and the OCR value at 1.20 under a swelling pressure
218 of 7.11 MPa. Zhang et al. [16] investigated the shear strength of intact COx claystone by carrying out
219 triaxial compression tests and found that the internal friction angle of intact COx claystone was about
220 24° . From the over-consolidation ratio and the effective internal friction angle, the K_0 value was
221 estimated at 0.64. Substituting the swelling pressure in the direction perpendicular to the stratification

222 and K_0 value into Eq. (7) yields the mean swelling pressure ($P_{s\text{-mean}}$ in MPa):

223
$$P_{s\text{-mean}} = P_{s\text{-per}} \frac{1+2K_0}{3} \quad (7)$$

224 The estimated mean swelling pressure of intact COx claystone was 5.39 MPa, which was quite close
225 to the value of 4.9 MPa indirectly determined from the swelling pressure tests on the
226 bentonite/claystone mixtures. This confirmed the reliability of the assumptions made above and the
227 relevance of the identified swelling mechanism for claystone in its mixtures with bentonite. Upon
228 hydration, the bentonite grains in the mixtures would swell rapidly due to their high swelling capacity
229 while the claystone grains adsorbed water and then swelled or collapsed under the pressure applied
230 by the previously swollen bentonite. The identified mechanism can be extended to other binary
231 mixtures composed of two clays with extremely different swelling capacities.



232
233 **Fig. 7** Swelling pressure versus claystone void ratio of intact claystone (modified after Zhang et al.
234 [19])

235 4 Conclusions

236 The swelling pressures of MX80 bentonite/COx claystone mixtures with various bentonite fractions
237 and dry densities were experimentally investigated in the laboratory. By considering the interaction

238 between bentonite and claystone grains during hydration, the claystone void ratio in the mixtures after
239 hydration was estimated based on the relationship between the swelling pressure and dry density of
240 pure bentonite. Comparison of the claystone void ratio after hydration with the initial one allowed the
241 volumetric strains of claystone grains under different stresses to be obtained. It was found that the
242 volumetric strain decreased linearly with the increase of pressure applied by the swollen bentonite.
243 According to this relationship, the mean swelling pressure of claystone grain was indirectly
244 determined.

245 Additionally, the mean swelling pressure of claystone grain was estimated according to the
246 relationship between the void ratio and the swelling pressure in the direction perpendicular to the
247 stratification of intact COx claystone. The estimated value was found to be comparable to that
248 indirectly determined from the swelling pressure tests on bentonite/claystone mixtures. This
249 confirmed the identified swelling mechanism of COx claystone grain in its mixtures with bentonite:
250 the claystone grains adsorbed water under the pressure applied by the previously swollen bentonite.

251 Notably, the swelling pressure of claystone with a specified water content was determined in this
252 study. The influence of initial water content on the swelling pressure of claystone powders will be
253 investigated in further studies.

254

255 **Acknowledgments**

256 The authors thank the Chinese Scholar Council (CSC) and the French Radioactive Waste
257 Management Agency (Andra) for the financial supports.

258

259 **References**

- 260 1. Andra (2005). Dossier 2005 Argile - Synthesis: Evaluation of the Feasibility of a Geological
261 Repository in an Argillaceous Formation (Meuse/ Haute-Marne Site). French National
262 Radioactive Waste Management Agency, Chatenay-Malabry CEDEX 241 pp. Accessed 22
263 November 2018
- 264 2. Agus SS, Schanz T (2008) A method for predicting the swelling pressure of compacted bentonites.
265 *Acta Geotech* 3(2): 125
- 266 3. Karnland O, Nilsson U, Weber H, Wersin P (2008) Sealing ability of Wyoming bentonite pellets
267 foreseen as buffer material–laboratory results. *Phys Chem Earth Parts A/B/C* 33: S472–S475
- 268 4. Komine H, Ogata N (1994) Experimental study on swelling characteristics of compacted bentonite.
269 *Can Geotech J* 31(4): 478–490
- 270 5. Komine H, Ogata N (1999) Experimental study on swelling characteristics of sandbentonite
271 mixture for nuclear waste disposal. *Soils Found* 39(2): 83–97
- 272 6. Mayne PW, Kulhawy FH (1982) Ko-OCR Relationships in Soil. *Journal of the Soil Mechanics and*
273 *Foundations Division* 108(6): 851-872
- 274 7. Middelhoff M, Cuisinier O, Masrouri F, Talandier J, Conil N (2020) Combined impact of selected
275 material properties and environmental conditions on the swelling pressure of compacted
276 claystone/bentonite mixtures. *Appl Clay Sci* 184: 105389
- 277 8. Mohajerani M, Delage P, Monfared M, Tang AM, Sulem J, Gatmiri B (2011) Oedometric
278 compression and swelling behaviour of the Callovo-Oxfordian argillite. *Int J Rock Mech Min*
279 *Sci* 48(4): 606-615

- 280 9. Sun DA, Cui H, Sun WJ (2009) Swelling of compacted sand-bentonite mixtures. *Appl Clay Sci*
281 43(3–4): 485–492
- 282 10. Tang CS, Tang AM, Cui YJ, Delage P, Schroeder C, De Laure E (2011) Investigating the pressure
283 of compacted crushed-Callovo-Oxfordian claystone. *Phys Chem Earth Parts A/B/C* 36(17-18):
284 1857-1866
- 285 11. Wang Q, Tang AM, Cui YJ, Delage P, Gatmiri B (2012) Experimental study on the swelling
286 behaviour of bentonite/claystone mixture. *Eng Geol* 124: 59–66
- 287 12. Yang LA, Tan TS, Tan SA, Leung CF (2002) One-dimensional self-weight consolidation of a
288 lumpy clay fill. *Géotechnique* 52(10): 713-725
- 289 13. Zeng ZX, Cui YJ, Zhang F, Conil N, Talandier J (2019) Investigation of swelling pressure of
290 bentonite/claystone mixture in the full range of bentonite fraction. *Appl Clay Sci*
291 <https://doi.org/10.1016/j.clay.2019.105137>
- 292 14. Zeng ZX, Cui YJ, Conil N, Talandier J (2020a) Effects of technological voids and hydration time
293 on the hydro-mechanical behaviour of compacted bentonite/claystone mixture. *Géotechnique*
294 <https://doi.org/10.1680/jgeot.19.P.220>
- 295 15. Zeng ZX, Cui YJ, Conil N, Talandier J (2020b) Experimental Investigation and Modeling of the
296 Hydraulic Conductivity of Saturated Bentonite–Claystone Mixture. *Int J Geomech*
297 [https://doi.org/10.1061/\(ASCE\)GM.1943-5622.0001817](https://doi.org/10.1061/(ASCE)GM.1943-5622.0001817)
- 298 16. Zhang CL, Czaikowski O, Rothfuchs T (2010) Thermo-Hydro-Mechanical behaviour of the
299 Callovo-Oxfordian clay rock. In: Final report
- 300 17. Zhang CL, Wieczorek K, Xie ML (2010) Swelling experiments on mudstones. *J Rock Mech*

- 301 Geotech Eng 2(1): 44-51
- 302 18. Zhang CL, Kröhn KP (2019) Sealing behaviour of crushed claystone–bentonite mixtures.
- 303 Geomech Energy Environ 17: 90-105
- 304 19. Zhang F, Cui YJ, Conil N, Talandier J (2020) Assessment of swelling pressure determination
- 305 methods with intact Callovo-Oxfordian claystone. Rock Mech Rock Eng 53(4): 1879-1888